International Journal of Information, Control and Computer Sciences
ISSN: 2517-9942
Vol:8, No:3, 2014

Performance Analysis of Brain Tumor Detection Based On Image Fusion

S. Anbumozhi, P. S. Manoharan

***Abstract*—**Medical Image fusion plays a vital role in medical field to diagnose the brain tumors which can be classified as benign or malignant. It is the process of integrating multiple images of the same scene into a single fused image to reduce uncertainty and minimizing redundancy while extracting all the useful information from the source images. Fuzzy logic is used to fuse two brain MRI images with different vision. The fused image will be more informative than the source images. The texture and wavelet features are extracted from the fused image. The multilevel Adaptive Neuro Fuzzy Classifier classifies the brain tumors based on trained and tested features. The proposed method achieved 80.48% sensitivity, 99.9% specificity and 99.69% accuracy. Experimental results obtained from fusion process prove that the use of the proposed image fusion approach shows better performance while compared with conventional fusion methodologies.

***Keywords*—**Image fusion, Fuzzy rules, Neuro-fuzzy classifier.

I. Introduction

MEDICAL image processing has developed as one of the critical factors in regular clinical applications, such as disease diagnosis and treatment planning. Owing to the technical limitations, the quality of medical images is usually unsatisfactory, degrading the accuracy of human interpretation and further medical image analysis, thereby, requiring the quality of these images to be enhanced. One approach to enhance the image quality is by image denoising. Several denoising approaches, like adaptive filters, wavelet-based methods, etc. were proposed. Another efficient technique is by image fusion which improves the image quality by combining the corresponding information from multimodal images into a single fused image. This resulting image is called as fused image.

A fusion process is nothing but a combination of salient information in order to synthesize an image with more information than individual image and synthesized image is more suitable for visual perception. Image fusion is a process of combining multiple input images of the same scene into a single fused image, which preserves full content information and also retaining the important features from each of the original images. The fused image should have more useful information content compared to the individual image.

Radiologists mostly prefer both MR and CT images side by side, when both images are available. This provides them all the available image information, but its accessibility is limited to visual correlation between the two images. Both CT and MR images can be employed as it is difficult to determine whether narrowing of a spinal canal is caused by a tissue or bone. Both the CT and MR modalities provide complementary information. In order to properly visualize the related bone and soft tissue structures, the images must be mentally aligned and fused together. This process leads to more accurate data interpretation and utility. In fundamental multi-modal image fusion methodologies, the source image is just overlaid by assigning them to different color channels. In color image fusion, this overlay approach is used to expand the amount of information over a single image, but it does not affect the image contrast or distinguish the image features.

So in this paper we propose a novel region based image fusion algorithm for multifocus and multimodal images which also overcomes the limitations of different approaches.

S.Anbumozhi is with Raja College of Engineering & Technology, Madurai, India (e-mail: anbumozhi.123@gmail.com).

P. S. Manoharan is with Thiagarajar College of Engineering, Madurai, India (e-mail:psmeee@tce.edu).

II. Related Work

An image fusion technique based on discrete wavelet transform using high boost filtering was proposed in T. Zaveri, and M. Zaveri [1]. The proposed algorithm achieved an accurate segmentation for region-based fusion using graph based normalized cut algorithm. The regions were extracted from the input registered source images using the resultant segmented image. Then the extracted regions were processed to fuse different regions using different fusion rules. The method was implemented on various registered images of multi-focus and multimodality categories and the fusion results were compared using standard reference based and non-reference based image fusion parameters. It has been observed from simulation results that the algorithm was consistent and preserved more information compared to earlier reported pixel based and region based fusion methods.

Tsagaris et al. [2] proposed a scheme for hyperspectral image fusion based on principal components transformation (PCT). The first principal component of each subgroup is used for image visualization. The number of bands in each subgroup depends on the application. However, in their work, three subgroups were used for RGB representation. One of the subgroups employed matched filtering based on the spectral characteristics. The quality of the obtained RGB images were quantitatively evaluated using parameters like, correlation coefficient, the entropy, and the maximum energy-minimum correlation index. The performance of their method in classification has been tested using the K-means algorithm.

Bhatnagar et al. [3] presented a fusion technique based on Non-Sub sampled Contourlet Transform (NSCT). The source medical images are first transformed by NSCT followed by

combining low frequency and high-frequency components. Two different fusion rules based on phase congruency and directive contrast are proposed and used to fuse low- and high-frequency coefficients. Finally, the fused image is constructed by the inverse NSCT with all composite coefficients. Experimental results and comparative study show that the proposed fusion framework provides an effective way to enable more accurate analysis of multimodality images. Further, the applicability of the proposed framework is carried out by the three clinical examples of persons affected with Alzheimer, sub-acute stroke and recurrent tumor.

A. Rana, and S. Arora [4] explored different medical image fusion methods and their comparison to find out which fusion method gives better results based on the performance parameters. Here medical images of magnetic resonance imaging (MRI) and computed tomography (CT) images are fused to form new image. In this paper, wavelet transform, principle component analysis (PCA) and Fuzzy Logic techniques are utilized for fusing these two images and results are compared. The fusion performance is evaluated on the basis of root mean square error (RMSE), peak signal to noise ratio (PSNR) and Entropy (H).

Pinki Jain and Anu Aggarwal [5] fused text data with medical images. In their work, the area of interest (AOI) for a particular image is found out and the text data of the patient is appended/fused in the non-area of interest (NAOI) of the image. They proposed a fusion rule based on matrix scanning to find the AOI and then finds the noisy pixels of the image to embed data in that noisy portions to save the border size. Their system used MATLAB for implementation and to store text data in pixels.

Sapkal and Kulkarnian [6] proposed an image fusion algorithm based on Wavelet Transform. It includes multi resolution analysis ability in Wavelet Transform. The method applies pixel-based algorithm for approximations involving fusion based on taking the maximum valued pixels from approximations of source images. Based on the maximum pixel values, a binary decision map is formulated. Then inverse wavelet transform is applied to reconstruct the resultant fused image and display the result. The wavelet sharpened images have a very good spectral quality.

Neha Tirpude, and Rashmi Welekar [9] proposed to extract the tumor portion and to diagnose whether the tumor is present or absent along with the exact size of the tumor. A fuzzy clustering based technique is proposed to study and analyze the intricate structure of the brain.

C. Gonzalez et al. [10] presented the role of hardware accelerators in hyperspectral remote sensing missions and further inter-comparing two types of solutions: Field programmable gate arrays (FPGAs) and graphics processing units (GPUs) is done. A full spectral unmixing chain is implemented and tested in their work.

N. Jacobson et al. [11] proposed methods to display hyperspectral image sets by linearly projecting them onto basis functions designed for the red, green, and blue (RGB) primaries of a standard tristimulus display, for the human visual system, and for the signal-to-noise ratio of the dataset, creating a single color image. Projecting the data onto three basic functions reduces the information but allows each data point to be rendered by a single color.

III. Proposed Fusion Algorithm

Fig. 1 shows the block diagram of the proposed fusion algorithm. It consists of a wavelet decomposition block, fusion circuit based on fuzzy logic, Feature extraction and Classifier for tumor detection. The features considered in our algorithm are Wavelet features, Energy features, correlation and Homogeneity features, and Contrast features, as depicted in Fig. 2.

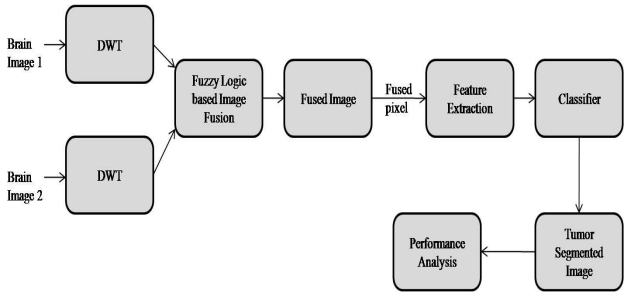

Fig. 1 Block diagram of proposed fusion process

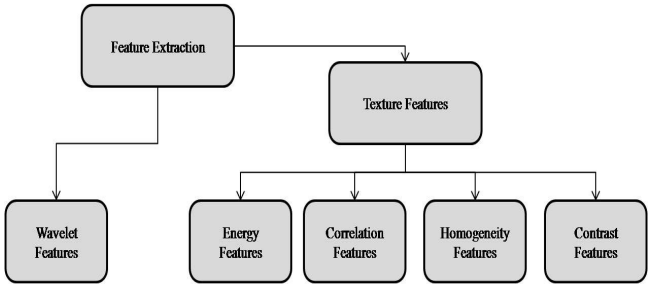

Fig. 2 Feature extraction circuit

A. Wavelet Decomposition

Image fusion using wavelet scheme decomposes the source images Image1 and Image2 into approximation and detailed coefficients at required level using DWT. The approximation and detailed coefficients of both images are combined using fusion rule. Based on the maximum valued pixels between the approximations, a binary decision map is generated gives the decision rule for fusion of approximation coefficients in the two source images.

IV. Feature Extraction

A. Wavelet Features

This is a texture related feature which is formed by the construction of wavelets from the brain MRI. Wavelets are small waves and are mathematical functions that represent scaled and shifted copies of a finite-length waveform called the mother wavelet.

$$\psi_{a,b}(t) = \frac{1}{\sqrt{a}}\psi\left(\frac{t-b}{a}\right) \quad (1)$$

where a is the scaling parameter and b is the shifting parameter.

A wavelet transform (WT) entirely depends on wavelets. WT analyzes the image on different resolution scales and splits the image into various frequency components, i.e. multi-resolution image. This permits to view the spatial and frequency attributes of the image simultaneously.

The wavelet is discontinuous, and resembles a step function. For a function f, the Haar WT is defined as:

$$f \rightarrow (a^L \mid d^L) \tag{2}$$

where, L is the decomposition level, a is the approximation sub-band and d is the detail sub-band.

Firstly, wavelet transform is applied to each row and secondly to each column of the resulting image of the first operation. The resulting image is decomposed into four sub-bands: LL, HL, LH, and HH sub-bands. (L=Low, H=High). The LL-sub-band contains an approximation of the original image while the other sub-bands contain the missing details. The LL-sub-band output from any stage can be decomposed further. Fig. 3 shows the result of pyramid decomposition.

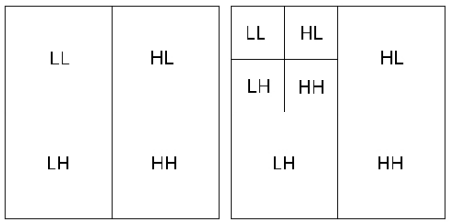

(a) (b)

Fig. 3 Pyramid Decomposition using discrete wavelet transform: (a) Decomposition at Level 1, (b) Decomposition at Level 2

B. Energy Texture Features

In this feature set, the 1D kernels of the brain image are converted into 2D filter kernels at the first step. Then, the input mammogram image is filtered with Law's 2D kernels and the energy features of the image are calculated:

$$Energy = \sum_i \sum_j P^2(i,j) \tag{3}$$

C. Correlation-Based Features

This feature relies on a heuristic for evaluating the worth or merit of a subset of features. This heuristic takes into account the usefulness of individual features for predicting the class label along with the level of inter-correlation among them. A feature is useful if it is correlated with or predictive of the class; otherwise it is irrelevant. Empirical evidence from the feature selection literature shows that, along with irrelevant features, redundant information should be eliminated as well.

If the correlation between each of the components in a test and the outside variable is known, and the inter-correlation between each pair of components is given, then the correlation between a composite consisting of the summed components and the outside variable can be predicted as,

$$Correlation = \sum_i \sum_j \frac{P(i,j)(i-\mu_i).(j-\mu_j)}{\sigma_i.\sigma_j} \tag{4}$$

where, μ_i, μ_j = mean correlation between the summed components and the outside variable, and σ_i, σ_j = variance between components.

D. Contrast and Homogeneity based Features

The co-occurrence based texture features using the Gray-Level Co-occurrence Matrices (GLCM) were defined by Haralick et al. [12]. GLCM is a matrix that shows the frequency of adjacent pixels with grayscale values *i* and *j*. For example, let matrix *I* be the grayscale values of image *I*, and (*i*, *j*) denotes a possible pair of the horizontally adjacent pixels *i* and *j*.

$$I = \begin{bmatrix} 0 & 0 & 1 & 1 \\ 0 & 2 & 1 & 1 \\ 0 & 2 & 2 & 2 \\ 2 & 2 & 1 & 0 \end{bmatrix} \tag{5}$$

$$where \ (i,j) = \begin{bmatrix} (0,0) & (0,1) & (0,2) \\ (1,0) & (1,1) & (1,2) \\ (2,0) & (2,1) & (2,2) \end{bmatrix}$$

GLCM represents the frequency of all possible pairs of adjacent pixel values in the entire image. For instance, in the GLCM for image *I* (i.e. $GLCM_I$), there is only one occurrence of two adjacent pixel values both being 0 (i.e. (0, 0)), whereas the frequency of having (0, 2) pixel values in image *I* is two, and so on.

$$GLCM_I = \begin{bmatrix} 1 & 1 & 2 \\ 1 & 2 & 0 \\ 0 & 2 & 3 \end{bmatrix} \tag{6}$$

From the resulting GLCM, the probability of having a pair of pixel values (*i*, *j*) occurring in each image (i.e. *P*(*i*, *j*)) is estimated. For example, the probability of having a pair of pixel values (0,0) in image *I* is 1/12, and the probability of having pixels (0,2) is 2/12.

The GLCM contrast and GLCM homogeneity are defined as follows,

$$GLCM\ Contrast = \sum_i \sum_j (i-j)^2 P(i,j) \tag{7}$$

$$GLCM\ Homogeneity = \sum_i \sum_j \frac{P(i,j)}{1+|i-j|} \tag{8}$$

GLCM contrast measures the variance in grayscale levels across the image, whereas GLCM homogeneity measures the similarity of grayscale levels across the image. Thus, the larger the changes in grayscale, the higher the GLCM contrast and the lower the GLCM homogeneity is found. Finally, GLCM energy measures the overall probability of having

distinctive grayscale patterns in the image. The extracted features are trained and tested by adaptive neuro-fuzzy algorithm.

V. ANFIS Classifier

Adaptive Neuro Fuzzy Interference Systems (ANFIS) are adaptive networks implemented in MATLAB software. An adaptive network consists of a group of nodes and directional links. The network has a learning rule such as back propagation. ANFIS is said to be adaptive because some or all the nodes have parameters which influences the output node. ANFIS is a supervised learning technique and relates the inputs with the outputs.

The ANFIS architecture is shown in Fig. 4. The circular nodes in the figure are fixed nodes and the square nodes have parameters to be trained.

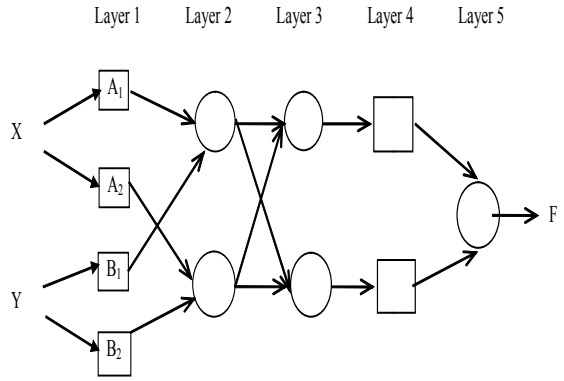

Fig. 4 ANFIS architecture for a two rule system

Consider an ANFIS classifier based on a Two-rule system as below,

If x is A1 and y is B1 then, f1=p1x+q1y+r1
If x is A2 and y is B2 then, f2=p2x+q2y+r2

For the training of the network, there is a forward pass and a backward pass. We now look at each layer in turn for the forward pass. The forward pass propagates the input vector through the network layer by layer. In the backward pass, the error is sent back through the network in a similar manner to back propagation.

VI. Results and Discussions

The original image and the fused image are compared by the quality metrics such as PSNR (Peak Signal to noise ratio), MMSE (Minimum mean square error), entropy and elapsed time. Our proposed fusion method is quantitatively evaluated and compared in terms of subjective testing, i.e., visual quality, where recommended parameters are used. For the quantitative testing of the fused images, we make use of the peak signal-to-noise ratio (PSNR) which is a prime evaluation factor. From the results, it is observed that our proposed fusion methodology performs very well.

The values of PSNR and MSE are represented mathematically as given below:

$$PSNR = 20\log_{10}\frac{MAX_f}{\sqrt{MSE}} \quad (4)$$

$$MSE = \frac{1}{mn}\sum_0^{m-1}\sum_0^{n-1}\|f(i,j) - g(i,j)\|^2 \quad (5)$$

where, 'm' represents width of the fused image and 'n' represents height of the fused image

$$Entropy = -\sum p * log(p) \quad (6)$$

where, 'p'represents histogram counts of each pixel value in an fused brain image.

Table I illustrates the variation of PSNR, MSE and Entropy, and Table II shows the time taken for fusion. Figs. 5 and 6 graphically represent the variation of PSNR, MSE and Entropy, and elapsed time variation in fusion, respectively.

TABLE I
Performance Comparison of Proposed Fusion Method in Terms of Quality Metrics

Methodology	PSNR (dB)	MSE	ENTROPY
Proposed Methodology	68.75	24.5	3.0
Group-Sparse Algorithm [8]	29.54	32.56	1.7864
Bivariate Laplacian mixture model [7]	22.16	37.19	1.9652

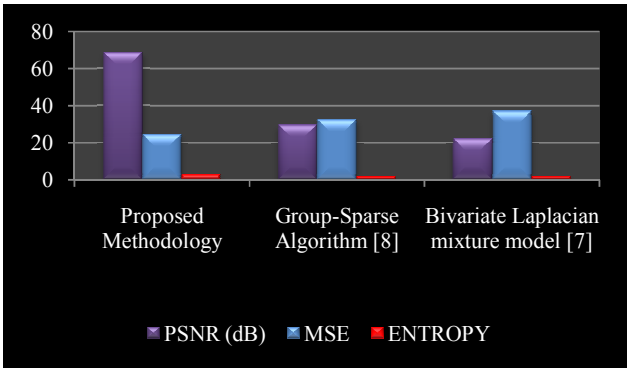

Fig. 5 Graphical illustration of performance comparison in terms of PSNR, MSE and Entropy

TABLE II
Performance Comparison of Proposed Fusion Method in Terms of Fusion Latency

Methodology	Elapsed Latency (s)
Proposed Methodology	0.13
Group-Sparse Algorithm [8]	0.38
Bivariate Laplacian mixture model [7]	0.45

The proposed method is evaluated for its performance in classification in terms of sensitivity, specificity and accuracy. These performance parameters are evaluated and tabulated in Table III.

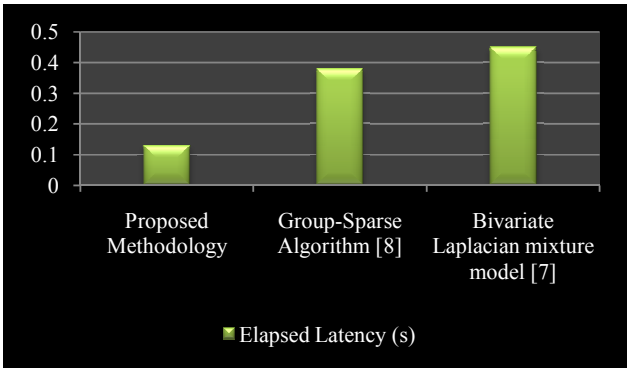

Fig. 6 Graphical illustration of comparison of Latency

TABLE III
PERFORMANCE ANALYSIS OF PROPOSED METHOD

Performance Parameters	Results
Sensitivity	80.48
Specificity	99.9
Accuracy	99.69

The proposed fusion method has been implemented over two different set of images, i.e., image set 1 and image set 2. The results of simulation are given in Table IV. Fig. 7 shows the simulation screenshot for VLSI implementations using Xilinx 9.2i tool and its RTL, Technology schematic visions. The test images and simulation output images, fused images and tumor identified images are shown in Figs. 8, 9 and 10 respectively.

TABLE IV
PERFORMANCE EVALUATION OF PROPOSED FUSION METHOD

Image Set	PSNR (dB)	MSE	Detection Latency (s)
Image Set 1 (Malignant)	68.71	23	172
Image Set 2 (Benign)	67.80	26	170

TABLE V
POST LAYOUT RESULTS OF PROPOSED ARCHITECTURE

Performance Parameters	Results
Technology	CMOS 90nm
Gate Count	5006
Power Consumption	69mW
Memory Size	151644KB

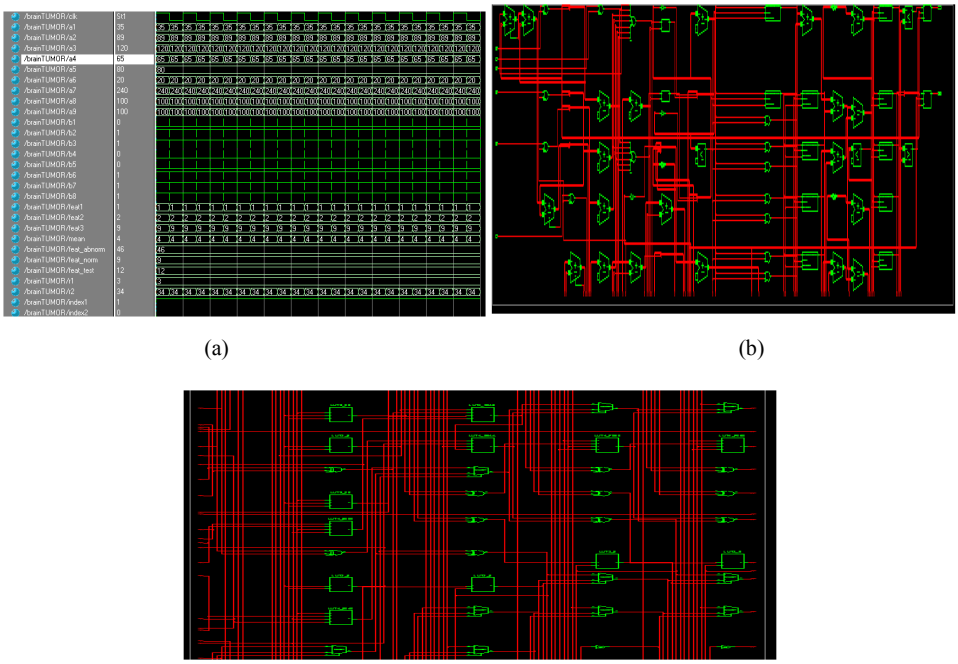

(a) (b)

(c)

Fig. 7 VLSI Architectures (a) Simulation Screenshot, (b) RTL Schematic, (c) Technology Schematic

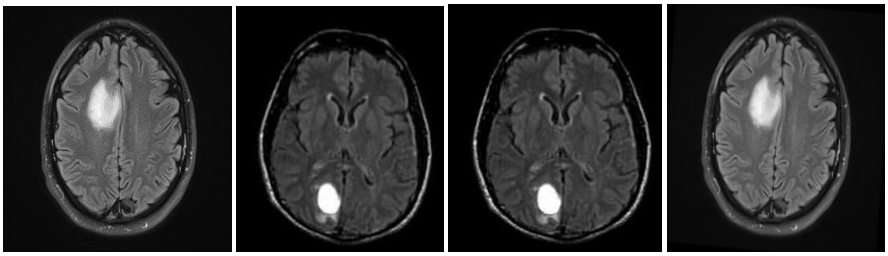

Fig. 8 Test images used in our proposed work

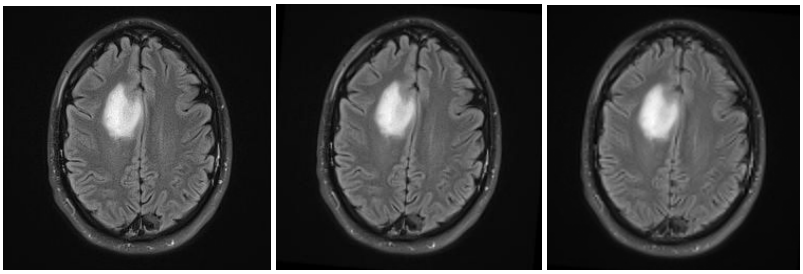

(a) (b) (c)

Fig. 9 Benign image fusion: (a) Brain image1, (b) Brain image2, (c) Fused image (Benign)

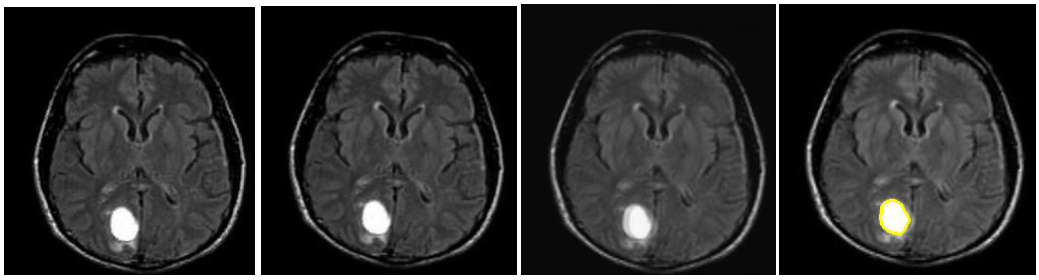

(a) (b) (c) (d)

Fig. 10 Malignant image fusion: (a) Brain image1, (b) Brain image2, (c) Fused image, (d) Tumor segmented image (Malignant)

VII. Conclusion

Medical image fusion combines different modality of medical images to produce a high quality fused image with spatial and spectral information. The fused image with more information improved the performance of image analysis algorithms used in different medical diagnosis applications. Fuzzy logic is used in this paper for brain image fusion and GLCM features are extracted from the fused brain image. The brain tumor region is segmented using the extracted features and adaptive neuro fuzzy classifier helps to identify whether the tumor is benign or malignant. Thus it helps the physician and radiologist for brain tumor diagnosis for human surgery.

References

[1] T. Zaveri, and M. Zaveri, "A Novel Region Based Multimodality Image Fusion Method", *Journal of Pattern Recognition Research*, vol. 2, pp. 140–153, 2011.

[2] V. Tsagaris, V. Anastassopoulos, and G. Lampropoulos, "Fusion of hyperspectral data using segmented PCT for enhanced color representation", *IEEE Trans. Geosci. Remote Sens.*, vol. 43, no. 10, pp. 2365–2375, 2005.

[3] G. Bhatnagar, Q. M. J. Wu, and Z. Liu, "Directive Contrast Based Multimodal Medical Image Fusion in NSCT Domain. *IEEE Transactions on Multimedia*, vol. 15, no. 5, pp. 1014–1024, 2013. DOI: 10.1109/TMM.2013.2244870.

[4] A. Rana, and S. Arora, "Comparative Analysis of Medical Image Fusion. *International Journal of Computer Applications*," vol. 73, no. 9, pp.10–13, 2013. DOI: 10.5120/12768-9371.

[5] Pinki Jain, and Anu Aggarwal, "Text Fusion in Medical Images using Fuzzy Logic based Matrix Scanning Algorithm," *International Journal of Scientific and Research Publications*, vol. 2, no. 6, pp. 1-6, 2012.

[6] R. J. Sapkal, and S. M. Kulkarni, "Image Fusion based on Wavelet Transform for Medical Application," *International Journal of Engineering Research and Applications*, vol. 2, no. 5, pp. 624-627, 2012.

[7] H. Rabbani, R. Nezafat, and S. Gazor, "Wavelet-domain medical image denoising using bivariate Laplacian mixture model," *IEEE Transactions on Biomedical Engineering*, vol. 56,no. 12,pp. 2826–2837, 2009. DOI: 10.1109/TBME.2009.2028876.

[8] S. Li, H. Yin, and L. Fang, "Group-Sparse representation with Dictionary Learning for Medical Image Denoising and Fusion. *IEEE Transactions on Biomedical Engineering*," vol. 59, no. 12, pp. 3450-3459, 2012. DOI: 10.1109/TBME.2012.2217493.

[9] Neha Tirpude, and Rashmi Welekar, "Automated Detection and Extraction of Brain Tumor from MRI Images", *International Journal of Computer Applications* (0975 – 8887), vol. 77, no. 4, September 2013.

[10] C. Gonzalez, S. Sanchez, Abel Paz, J. Resano, D. Mozos, and A. Plaza, "Use of FPGA or GPU-based architectures for remotely sensed

hyperspectral image processing," *INTEGRATION, The VLSI Journal*, vol. 46, no. 2, pp. 89–103, March 2013.
[11] N. Jacobson, M. Gupta, and J. Cole, "Linear fusion of image sets for display," *IEEE Trans. Geosci. Remote Sens*., vol. 45, pp. 3277– 3288, 2007.
[12] R. M. Haralick, K. Shanmugan, and I. Dinstein, "Textural Features for Image Classification", *IEEE Transactions on Systems, Man, and Cybernetics*, vol. SMC-3, pp. 610-621, 1973.